



Published in final edited form as:

Cancer Res. 2018 June 15; 78(12): 3207–3219. doi:10.1158/0008-5472.CAN-18-0222.

Silencing of long non-coding RNA *MIR22HG* triggers cell survival/death signaling via oncogenes *YBX1*, *MET*, and *p21* in lung cancer

Wenmei Su^{1,2}, Shumei Feng³, Xiuyuan Chen⁴, Xia Yang⁵, Rui Mao³, Chunfang Guo², Zhuwen Wang², Dafydd G. Thomas⁶, Jules Lin², Rishindra M. Reddy², Mark B. Orringer², Andrew C. Chang², Zhixiong Yang¹, David G. Beer², and Guoan Chen²

¹Department of Oncology, Affiliated Hospital of Guangdong Medical University, Zhanjiang, China

²Section of Thoracic Surgery, Department of Surgery, University of Michigan, Ann Arbor, Michigan, USA

³Xinjiang Medical University, Urumqi, China

⁴Peking University People's Hospital, Beijing, China

⁵Xian Jiaotong University, Xi'an, China

⁶Department of Pathology, University of Michigan, Ann Arbor, USA

Abstract

The long non-coding RNA (lncRNA) *MIR22HG* has previously been identified as a prognostic marker in hepatocellular carcinoma. Here we performed a comprehensive analysis of lncRNA expression profiles from RNA-seq data and report that *MIR22HG* plays a similar role in lung cancer. Analysis of 918 lung cancer and normal lung tissues and lung cancer cell lines revealed that *MIR22HG* was significantly downregulated in lung cancer; this decreased expression was associated with poor patient survival. *MIR22HG* bound and stabilized the *YBX1* protein. Silencing of *MIR22HG* triggered both cell survival and cell death signaling through dysregulation of the oncogenes *YBX1*, *MET*, and *p21*. In this *MIR22HG* network, *p21* played an oncogenic role by promoting cell proliferation and anti-apoptosis in lung cancers. *MIR22HG* played a tumor suppressor role as indicated by inhibition of multiple cell cycle-related genes in human primary lung tumors. These data show that *MIR22HG* has potential as a new diagnostic and prognostic marker and as a therapeutic target for lung cancer.

Significance—The lncRNA *MIR22HG* functions as a tumor suppressor with potential use as a diagnostic/prognostic marker and therapeutic target in lung cancer.

Address correspondence to: Guoan Chen, University of Michigan, 1500 E. Medical Center Drive, Ann Arbor, Michigan 48109, Phone: 734-647-2787; guoanche@umich.edu; Zhixiong Yang, Guangdong Medical University, yangzhixiong1963@hotmail.com.

Disclosure of Potential Conflicts of Interest

No potential conflicts of interest were disclosed.

Introduction

Approximately 80% of lung cancers are non-small cell lung cancer (NSCLC), which includes adenocarcinoma (AD) and squamous cell carcinoma (SCC) and represent a leading cause of cancer-related deaths (1). The poor prognosis and high recurrence rate of lung cancer is largely due to the high rate of metastases and complex cellular, molecular and tumor micro-environmental factors (2,3). Despite the emergence of new adjuvant therapy regimens and targeted biologic agents, the 5-year survival rate of NSCLC remains dismal at 18% (1). It is of paramount importance to understand the underlying pathological mechanisms contributing to NSCLC in order to develop novel diagnostic biomarkers and therapeutic strategies and improve survival (4,5).

Recent studies suggest that long non-coding RNAs (lncRNAs) are involved in the initiation and progression of cancer and are often highly deregulated in tumors (6–9). LncRNAs are operationally defined as transcripts that are larger than 200 nt without protein coding potential, and they have been shown to play vital roles in various aspects of cancer biology (10,11). Mounting evidence has shown that lncRNAs influence various cellular processes such as proliferation, cell cycle progression, cell proliferation, and apoptosis (12,13). LncRNAs have been found to act as tumor suppressors or oncogenes (14,15). In this regard, identifying cancer-associated lncRNAs and the molecular mechanisms they affect is necessary for understanding progression and establishing better treatments for NSCLC.

High-throughput RNA sequencing (RNA-Seq) in human cancers has shown a remarkable potential for identifying both novel markers of disease and uncharacterized aspects of tumor biology, particularly new lncRNA species (16,17). To define lncRNAs important for lung cancer, by analyzing three large sets of RNA-Seq data including TCGA, Seo and UM, we identified 281 lncRNAs with an ROC > 0.7 or < 0.25 which were listed in our previous publication (18). *MIR22HG* was one of the most down-regulated lncRNAs in lung cancer as compared to normal lung tissues, thus its biological functions and underlying molecular mechanisms in this disease were examined in this study.

Materials and Methods

Patient tissue samples and cell lines

The lung cancer and paired non-tumor lung tissues were obtained from patients undergoing curative cancer surgery during the period from 1991 to 2014 at the University of Michigan Health System. None of the patients included in this study received any preoperative radiation or chemotherapy. Written informed consents were obtained from subjects or their authorized representatives. The study protocol was approved by the University of Michigan Institutional Review Board and Ethics Committee. Resected specimens were frozen in liquid nitrogen and then stored at -80°C until use. The median follow-up time was 8.12 years among the patients that remained alive. The clinical information of LUAD samples used in qRT-PCR validation (101 LUADs) was in Supplementary Table S1.

Lung cancer cell lines (PC-9, H1975, H1299, H838 and H2228) were obtained from the American Type Culture Collection (Supplementary Table S2). All cell lines were genotyped

for identity at the University of Michigan Sequencing Core and were tested routinely for mycoplasma contamination using MycoAlert mycoplasma detection kit (Lonza). All cell lines were maintained in RPMI 1640 or EMEM supplemented with 10% FBS and 1% antibiotic-antimycotic agents and cultured at 37°C in a 5% CO₂ cell culture incubator. Cells were grown for no more than 25 passages in total for any experiment.

Published microarray and RNA sequencing data collections

Two published microarray data sets representing 668 primary lung AD tissues were downloaded from NCBI Gene Expression Omnibus (GEO) (GSE31210 and GSE68465). These included Okayama et al., 226 LUADs with stage 1 and 2 (19), and Shedden et al., with 442 stage 1 to 3 LUADs (20). The CEL files of microarray data were normalized using Robust Multi-array Average (RMA) method (21). We also obtained Seo (22) and TCGA (23) RNA-Seq data sets consisting of a total of 394 ADs, 212 SCCs and 150 normal lung tissues (<https://portal.gdc.cancer.gov>). Expression levels of transcripts were represented as FPKM (24). RNA-Seq of UM cohort (24) including 113 lung cancer tissues (67 LUADs, 36 SCCs, 10 large cell lung cancers and 6 normal) was also included in this analysis. Our primary outcome was overall survival, censored at five years. The information concerning adjuvant chemotherapy or radiation therapy was provided in the original papers.

siRNA-mediated knockdown

Cells were plated at a desired concentration and transfected with targeting siRNA oligonucleotides or non-targeting controls 2–24 h after plating with final concentration of 10 nM. Knockdown was performed with Lipofectamine® RNAiMax Reagent (Invitrogen) in OptiMEM medium according to the manufacturer's instructions. Knockdown efficiency was determined by qRT-PCR. All siRNAs were purchased from Dharmacon and the sequences used in this study are provided in Supplementary Table S3.

Cell proliferation assay and colony formation assay

Cells were plated in 96 well plates at a desired concentration and transfected with 10 nM experimental siRNA oligonucleotides or non-targeting controls at 2–24 h after plating. At 12 h, 24 h, 48 h, 72 h, 96 h, and 120 h after transfection with siRNA, the proliferation rates were measured by Cell Proliferation Reagent (WST-1) (Roche) according to manufacturer's instructions. The cell viability percentage was calculated by normalizing to the non-target control siRNA.

For colony formation, lung cancer cells transfected with *MIR22HG* siRNAs and control siRNA were seeded in a six-well plate at a density of 200 cells/well. After 10 to 14 days of incubation at 37 °C, 0.1% crystal violet (Sigma-Aldrich) and 20% methanol were used as dye solution to fix and stain the colonies. The number of colonies was counted in each well. Clones containing more than 50 cells were counted using a grid. Three independent experiments were performed.

RNA immunoprecipitation (RIP)

RIP assays were performed as described previously. RIP assays will be performed using a Millipore EZ-Magna RIP RNA-Binding Protein Immunoprecipitation kit (Millipore)

according to the manufacturer's instructions. Antibodies to be used for RIP are rabbit polyclonal IgG (Millipore) and YBX1 (Santa Cruz Biotechnology) using 5 µg of antibody per RIP reaction.

Statistical analysis

Data were analyzed using GraphPad Prism 6 (GraphPad software), Excel and R software. Receiver Operating Characteristic (ROC) curve and the area under the curve (AUC) analysis was used to show the tradeoff between sensitivity and specificity for the different possible cut-points of a diagnostic test. Kaplan-Meier survival curves with log-rank test was used for survival analysis. Heat maps were used to visualize the difference of gene expression using Tree View software. The other data such as proliferation were evaluated by unpaired Student's t-test. A two-tailed p value < 0.05 was considered significant. DAVID pathway analysis (25) was used to determine the potential biological processes associated with *MIR22HG* correlated genes.

Other materials and methods including RNAs extraction and quantitative real-time RT-PCR, proteins extraction, immunoblot analysis and tissue array, cell cycle analysis by flow cytometry, *MIR22HG* lentiviral expression construct transfection were detailed in Supplementary Methods.

Results

MIR22HG is decreased in lung cancer and associated with poor patient survival

In the current study, a comprehensive analysis of the gene expression data-matrix from three cohorts of RNA-seq data was performed to define differentially expressed lncRNAs in lung adenocarcinomas (LUAD). The three cohorts were two large publicly-available RNA-Seq data: the Korean cohort (Seo) (22), including 85 LUADs and 77 normal lung tissues; the Cancer Genome Atlas (TCGA) lung data (23), including 309 LUADs, 212 SCCs and 73 normal lung tissue samples; and the UM cohort, including 113 lung cancer tissues (67 LUADs, 36 SCCs, 10 large cell lung cancers and 6 normal) (24). *MIR22HG*, one of the top dysregulated lncRNAs, was found to be significantly reduced in LUAD as compared to normal lung tissues in Seo, TCGA and UM RNA-Seq datasets (Fig. 1A–C). Accordingly, Receiver Operating Characteristic (ROC) curve analysis was performed, and the area under the curve (AUC) values were larger than 0.94 in all three cohorts (Fig. 1D–F), indicating that *MIR22HG* may be potentially used as a novel diagnostic marker for this type of lung cancer. *MIR22HG* expression was also significantly lower in SCC and large cell lung cancer (LC) (Supplementary Fig. S1A and S1B). Next, where survival information was available, the association of *MIR22HG* expression and patient survival in two independent published LUAD microarray datasets, Okayama et al. (226 LUADs) (19) and Shedden et al. (442 LUADs) (20) was evaluated. Kaplan-Meier survival curves and log-rank tests showed that lower expression level of *MIR22HG* was significantly correlated with poor patient outcome in the Okayama data set (p = 0.02) and Shedden dataset (p = 0.02) (Fig. 1G and 1H). These data demonstrated that the downregulation of *MIR22HG* may play a tumor suppressor role in lung cancers and could be a novel diagnostic marker.

Validation of *MIR22HG* expression pattern in an independent cohort of LUADs by qRT-PCR and expression status in other types of cancer

To further verify the *MIR22HG* expression pattern discovered from RNA-Seq and microarray datasets, qRT-PCR assays using mRNA from an independent UM cohort including 101 LUADs and 27 normal lung tissues were performed. The qRT-PCR results showed that *MIR22HG* expression levels were significantly lower in LUAD as compared to normal lung tissues ($p < 0.001$) (Fig. 2A). The AUC was 0.79, indicating that *MIR22HG* expression level could separate the tumors from normal lung (Fig. 2B). Kaplan-Meier survival curve and log-rank test indicated that higher expression of *MIR22HG* was significantly associated with better patient survival ($p = 0.003$) (Fig. 2C). The relationship between *MIR22HG* expression and other clinical variables from this validation cohort was also analyzed. These clinical variables included age, gender, smoking status, tumor stage, lymph node status, differentiation and *KRAS* mutation status. It was found that *MIR22HG* level had a lower trend in Stage 3 (vs. Stage 1) NSCLC and in patients with positive lymph node metastasis (vs. N0) (Supplementary Table S1).

To determine if *MIR22HG* expression is associated with other types of cancer, we analyzed RNA-Seq expression data from the MiTranscriptome database, which contains 6,220 cancers (17). *MIR22HG* was found to be decreased in many types of cancer, including bladder, breast, gastric, head-neck, kidney and liver cancer (FPKM log₂ value, normal vs. cancer, t test, $p < 0.001$) (Fig. 2D). Interestingly, we found metastatic cancers of prostate and thyroid have even lower levels of *MIR22HG* as compared to their own primary cancer (Fig. 2E). These results indicated that *MIR22HG* expression is generally lower in most types of cancer and may be also an indicator of metastatic tumor.

We also analyzed *MIR22HG* expression levels in 33 lung cancer cell lines from RNA-Seq data (24). We found that *MIR22HG* was expressed in all 30 NSCLC cell lines, with lower expression in the small cell lung cancer cell lines, H146, H526 and H82 (Supplementary Fig. S2).

Cancer cell proliferation, colony formation, migration and invasion are increased after *MIR22HG* knockdown in lung cancers

The biological function of *MIR22HG* in lung cancer is poorly understood. To explore the possible role of *MIR22HG* in lung cancer pathogenesis, we used siRNA technology to knockdown *MIR22HG* expression in 5 lung cancer cell lines having different genomic backgrounds, including H1975 (*EGFR* T790 mutation), PC-9 (*EGFR* 19 exon deletion), H2228 (*EML4-ALK* fusion), H1299 (*TP53* mutation), and H838 (*TP53* mutation) (Supplementary Table S2). Using both RNA-Seq and qRT-PCR, we confirmed *MIR22HG* was expressed in these cell lines (Supplementary Fig. S3A and S3B). To minimize the possibility of off-target effects, we used SMART pool gene specific siRNAs including 4 different siRNAs. The knockdown efficiency was confirmed by qRT-PCR in these cells (Fig. 3A).

We then measured effects on cell proliferation using WST-1 assays after silencing of *MIR22HG* by siRNAs in these lung cancer cell lines. We found that the cell proliferation

was increased by 30%–70% as compared to control siRNA at 96–120 hrs (Fig. 3B). Colony formation assays further confirmed that cell proliferation was affected by *MIR22HG* knockdown (Fig. 3C; Supplementary Fig. S3C). Cell cycle analysis by flow cytometry indicated that the G1 phase was arrested in PC-9 cells, whereas G2 phase was arrested in H838 cells after *MIR22HG* knockdown with siRNA at 48 hrs (Supplementary Fig. S3D), indicating that the effects on cell cycle regulation were different in these cells. The possible reasons for why cell proliferation was increased but cell cycle was arrested are discussed in Discussion part. Trans-well assays were employed to evaluate whether cell invasion and migration were affected by *MIR22HG* in lung cancer cells. We found that cell invasion through matrigel-coated membranes significantly increased with *MIR22HG* knockdown as compared to the cells treated with non-target control siRNA (Fig. 3D; Supplementary Fig. S3E). Consistent with the invasion assay results, silencing of *MIR22HG* also significantly promoted cell migration (Fig. 3D; Supplementary Fig. S3E). These results suggested that *MIR22HG* is involved in lung cancer pathogenesis by affecting proliferation/cell cycle regulation, colony formation, invasion and migration.

To uncover the cellular localization of *MIR22HG*, we measured *MIR22HG* expression in both nuclear and cytoplasmic fractions from H1975, H838, PC-9 and H1299 cells by qRT-PCR. The differential enrichment of GAPDH for cytoplasmic and U1 for nuclear expressions were used as fractionation indicators. We observed that *MIR22HG* level was primarily in cytoplasm (61%–76%), and less in nuclear fractions (24%–39%) (Fig. 3E; Supplementary Fig. S3F). This suggested that *MIR22HG* may play a regulatory function mainly occurring in the cytoplasm.

***MIR22HG* knockdown decreases YBX1 and MET, but increases p21 expression**

To provide mechanistic insight into the role of *MIR22HG* in regulating lung cancer cells growth, we first performed receptor tyrosine kinase (RTK) phosphorylation antibody arrays, which include 49 different phosphorylated proteins, and confirmed by Western blot for proteins involved in major lung cancer-related pathways. We found that the MET and YBX1 proteins were significantly decreased, whereas p21 protein was increased after *MIR22HG* siRNA knockdown (Fig. 4A–C). Further, we found that these proteins were altered as early as 18–24 hours after *MIR22HG* knockdown (Fig. 4C). RT-PCR indicated that MET mRNA was significantly decreased in all tested cell lines (Fig. 4D) after *MIR22HG* knockdown suggesting that *MIR22HG* regulation of MET expression may be at the transcription level. YBX1 mRNA, however, was not changed after *MIR22HG* knockdown, indicating that YBX1 was regulated by *MIR22HG* at the protein level (Fig. 4E). The mRNA of p21 was increased by 20%–40% in H2228, H1975 and PC-9 cells, while not changed in H1299 and H838 cells (Fig. 4F), suggesting both transcriptional and translational regulation mechanisms for p21 by *MIR22HG* in these cells. Protein levels of AKT, ERK1/2, and STAT3 were not changed after *MIR22HG* knockdown (Supplementary Fig. S4A and S4B).

***MIR22HG* interacts with YBX1 protein and increases its stability**

We next examined how *MIR22HG* regulates YBX1, MET, and p21. It's reported that YBX1 can bind to the promoter of MET and regulate MET expression at both the mRNA and protein levels, and p21 could be also a potential target of YBX1 (26). Since YBX1 is a

RNA/DNA-binding protein, an important oncoprotein (27–29) and YBX1 mRNA was not changed after *MIR22HG* knockdown (Fig. 4E), we hypothesized that *MIR22HG* may regulate MET or p21 through affecting the YBX1 protein. To test the interaction between *MIR22HG* and YBX1 protein, we performed RNA immunoprecipitation (RIP) assays in which the RNA-YBX1 complex was immunoprecipitated using an YBX1 antibody. The amount of *MIR22HG* RNA in the co-precipitate was measured by qRT-PCR. As compared to the immunoglobulin G (IgG)-bound sample, we found that the YBX1-antibody-bound complex had a significant increase in the amount of *MIR22HG* indicating *MIR22HG* may directly interact with the YBX1 protein (Fig. 5A). YBX1 was degraded by the 20S proteasome in an ubiquitin- and ATP-independent manner and was abolished by the association of YBX1 with messenger RNA (30). To explore the role of *MIR22HG* in YBX1 protein regulation, we first treated PC-9 cells with the protein synthesis inhibitor, cycloheximide (CHX), followed by *MIR22HG* knockdown. We found that the half-life of YBX1 was much shorter in *MIR22HG* knockdown cells as compared to controls (Fig. 5B). Next, we treated with MG132, a proteasome inhibitor, to test whether decreased YBX1 is through proteasome degradation. We found that the endogenous YBX1 protein in *MIR22HG* knockdown cells was not decreased (Fig. 5C), indicating that YBX1 degradation may be through ubiquitin-conjugation mediated protein degradation. Together, these findings suggest that *MIR22HG* binds and stabilizes the YBX1 protein and through a *MIR22HG*-YBX1 complex to promote MET transcription and inhibit p21 expression (Fig. 5D).

In order to confirm YBX1 is regulated by *MIR22HG*, we performed YBX1 immunofluorescence staining on PC-9 cells after *MIR22HG* knockdown. We found YBX1 protein was present in both the cytoplasm and nucleus, and accumulated in nucleus at mitosis in control cells (Supplementary Fig. S5A), which was consistent with previous reports (31,32). Importantly, we found that the nuclear and cytoplasmic total YBX1 protein were significantly decreased upon *MIR22HG* knockdown suggesting that *MIR22HG* may not only affect total YBX1 degradation, but also affect YBX1 nuclear translocation.

To explore if MET, p21 or *MIR22HG* were affected by YBX1, we transfected YBX1 siRNA into PC-9, H1975, H1299, H838 and H2228 cells. We found that both MET protein and mRNA were decreased (Supplementary Figs. 5B, 5E and 5F), consistent with *MIR22HG* knockdown shown in Fig. 4, while p21 protein increased after YBX1 knockdown (Fig. 5E), which was similar to *MIR22HG* knockdown shown in Fig. 4. The change in p21 mRNA (increased in PC-9 and H1975, not changed in other cells) after YBX1 knockdown is also similar to *MIR22HG* knockdown (Fig. 4F; Supplementary Fig. S5C). We found that *MIR22HG* level was decreased upon YBX1 knockdown (Fig. 5G), indicating that *MIR22HG* expression was also affected by YBX1, perhaps through a positive feedback mechanism or directly regulating *MIR22HG* through targeting its promoter (Fig. 5D). Again, knockdown of YBX1 did not affect the expression of AKT, ERK1/2 and STAT3 protein levels (Supplementary Fig. S5D).

We have performed silencing of both *MIR22HG* and YBX1 to examine changes to the downstream proteins MET and p21 measured by Western blot. We found that *MIR22HG* has a stronger regulation on MET or p21 than YBX1 (Fig. 5H). Since YBX1 is involved in cancer progression (28), we tested whether YBX1 affects cell proliferation in lung cancer

cells. We found that cell proliferation was significantly decreased in PC-9 and H1975 cells after YBX1 knockdown but produced less than a 20% decrease in H2228, H1299 and H838 cells (Supplementary Fig. S5E), suggesting that YBX1 may only affect a subset of cancers by itself.

MET is also a well-known oncogene that can promote cell proliferation. We used siRNA to knockdown MET expression, with the efficiency of MET knockdown confirmed by qRT-PCR in H1975, PC-9, H1299 and H2228 cells (Supplementary Fig. S5F). Proliferation was decreased in the PC-9 and H1975, but was not changed significantly in H2228, H1299 and H838 cells (Supplementary Fig. S5G) after MET knockdown. We found that YBX1 protein/mRNA were increased slightly after MET knockdown in PC-9 and H1975 cells but not changed in H1299 and H2228 cells (Supplementary Figs. S5H and S5I), indicating that a negative feedback between MET and YBX1 may be present in some cells. Similarly, we found that p21 protein/mRNA was increased in PC-9, H1975 and H2228 cells, but not in H1299 cells (Supplementary Figs. S5H and S5J), suggesting that MET may inhibit p21 expression in a subset of tumor cells. We also found that MET knockdown did not change *MIR22HG* expression except in H1975 cells (Supplementary Fig. S5K). Proliferation was decreased or not changed by YBX1 or MET knockdown (decreased in PC-9 and H1975, but not significantly changed in H222, H1299 and H838 cells), which was opposite to *MIR22HG* knockdown where cell proliferation was increased in all of these five cell lines. These results indicate that the increased cell growth by *MIR22HG* knockdown is not due to YBX1 or MET knockdown, and the role of YBX1 or MET in regulation of cell proliferation is limited. We speculate that another protein, p21, may actually potentially play an oncogenic role in lung cancer, although p21 has been reported as a tumor suppressor gene (33,34).

p21 plays an oncogenic role in promoting tumor cell proliferation, anti-apoptosis and senescence

The p21 protein affects many biological processes (35) and can promote carcinogenesis and tumor progression (36,37). Cell proliferation was increased upon *MIR22HG* knockdown, but YBX1 and MET expression were decreased. Knocking down of YBX1 or MET decreased cell proliferation in PC-9 and H1975 cells, indicating that other protein, potentially increased p21, may be involved in processes regulated by *MIR22HG*. To test the effect of p21 on cell growth, we performed p21 knockdown with siRNAs against p21 in five lung cancer cell lines. The knockdown efficiency of p21 is large than 70% as compared to non-target control (Supplementary Fig. S6A). Surprisingly, we found that cell proliferation was dramatically decreased in all of these five cell lines (PC-9, H1975, H1299, H838 and H2228) after silencing of p21 by siRNA (Fig. 6A), indicating that p21 may play an oncogenic role in lung cancer. This is an agreement with our previous observation that *MIR22HG* knockdown significantly increased p21 expression (Figs. 4B and 4C) and promoted cell proliferation (Fig. 3B). In order to test if *MIR22HG* could rescue p21 in regulation of cell proliferation, we transfected *MIR22HG* siRNA, p21 siRNA or both siRNAs, respectively, into PC-9 and H838 cell lines. We found that the cell proliferation affected by p21 knockdown could be partially rescued by *MIR22HG* knockdown (Figs. 6B and 6C). This finding suggests that increased cell proliferation by *MIR22HG* knockdown

may be via p21 activation to decrease cell proliferation by decreased MET and YBX1 expression.

Cytoplasmic p21 has been found to be overexpressed in a variety of human cancers, including breast, cervical, prostate, renal, and testicular (38). Cytoplasmic localization of p21 was linked to anti-apoptotic actions, enhanced cell growth and survival, as well as acting as a chaperone for cyclin E (39). We found that the more abundant changes in protein expression of p21 and MET were in cytoplasm after *MIR22HG* knockdown in lung cancer cell lines (Supplementary Fig. S6B). Using the marker of apoptosis cleaved PARP, we observed decreased cleavage (along with increased p21, while p27 and TP53 were not changed) upon *MIR22HG* knockdown (Supplementary Fig. S6C), indicating an anti-apoptosis effect by *MIR22HG* knockdown perhaps through p21 activation. To confirm whether p21 may play an anti-apoptosis role and if *MIR22HG* can rescue this phenotype, we measured PARP cleavage after treatment with siRNAs specific to *MIR22HG*, p21 or both in PC-9, H1975 and H838 cells. We found that p21 knockdown led to a significant increase in cleaved PARP, and *MIR22HG* knockdown could rescue apoptosis (Fig. 6D). We also found that CCNE1 protein was decreased upon p21 knockdown, which is consistent with p21 acting as a chaperone for cyclin E (39) (Fig. 6E). In agreement with these findings, CCNE1 protein was increased after *MIR22HG* knockdown (Fig. 6F), indicating that up-regulation of CCNE1 by *MIR22HG* knockdown is through increased p21. This result demonstrates that increased cell growth by *MIR22HG* knockdown may be partially through p21 anti-apoptosis effects and promoting cell proliferation in lung cancer.

Following knockdown of p21, we found *MIR22HG* expression decreased, indicating that a positive feedback was present between p21 and *MIR22HG*, especially in H1299 and H838 cells (Supplementary Fig. S6D). A positive feedback was also present between p21 and phosphor-MET in H2228, PC-9 and H838 cells (Supplementary Fig. S6E).

MYC is reported to be inhibited by p21 (33), thus we tested whether MYC is involved in *MIR22HG* signaling. We found that MYC protein was slightly increased upon p21 knockdown (Supplementary Fig. S6E), which was consistent with *MIR22HG* knockdown (MYC was decreased) (Supplementary Fig. S6F), indicating that *MIR22HG* regulation of MYC may be also via p21. MYC mRNA was increased after p21 knockdown suggesting this regulation is at the transcriptional level especially in H1299, H1975 and H838 cells (Supplementary Fig. S6G). We didn't find TP53 was changed after *MIR22HG* knockdown (Supplementary Figs. S6B and S6F), although p21 was significantly increased (Figs. 4B and 4C; Supplementary Fig. S6B), indicating that *MIR22HG* regulation of p21 is independent of TP53. Knockdown of p21 also did not affect TP53 expression (Supplementary Fig. S6E).

To confirm the relationship between *MIR22HG* and p21, we transfected an *MIR22HG* overexpression construct into PC-9 and H1299 cell lines and found that p21 was markedly inhibited in expression (Figs. 6G and 6H; Supplementary Fig. S6H).

A recent report indicates that chronic overexpression of p21 (>10 days) acts as a powerful selection process, promoting both the escape of a subpopulation of cells from a senescence-like state and replication stress due to continuous re-replication (40). The key positive effects

and functions of p21 were found to correlate with both modulation of apoptosis and the induction of senescence (33). In fact, p21 was first identified as an overexpressed gene in normal human diploid senescent fibroblasts (41), and later found to induce premature senescence in human lung cancer H1299 cells (42). We performed two rescue experiments to confirm the relationship between *MIR22HG* and p21 by cell proliferation and apoptosis analysis shown previously (Figs. 6B–D). In order to examine whether the senescence phenotype induced by *MIR22HG* knockdown can be rescued by p21 knockdown, we transfected siRNAs specific to *MIR22HG*, p21, or both into PC-9 and H838 cells followed by measurement of β -galactosidase activity. We observed that the expression of *MIR22HG* siRNAs remarkably increased the number of cells with typical senescence morphology, whereas p21 knockdown decreased β -galactosidase activity (Supplementary Figs. S6I and S6J). Finally, knockdown of p21 expression rescued the senescence phenotype induced by *MIR22HG* siRNA. Together, these results indicate that *MIR22HG* exerts its function at least in part by regulating p21 expression.

Genes negatively correlated with *MIR22HG* are involved in cell cycle/proliferation regulation in primary lung cancer

In order to further understand the role of *MIR22HG* in human primary tumors, we performed Pearson correlation analysis between *MIR22HG* and 16,000 coding genes based on RNA-seq data from 3 cohorts including a total 461 LUADs (Seo 85 LUADs, UM 67 LUADs and TCGA 309 LUADs). There are 444 coding genes with negative correlation ($r < -0.35$, $p < 0.001$) and 168 with positively correlated coding genes ($r > 0.35$, $p < 0.001$) (Supplementary Fig. S7A). Using David gene annotation and pathway analysis, we found that the *MIR22HG* negative correlated genes were significantly involved in cell cycle regulation (Fig. 7A; Supplementary Figs. S7B and S7C). Among these *MIR22HG* negative-correlated genes, the cell proliferation marker, MKI67 (protein ki-67 coding gene), was significantly negatively correlated with *MIR22HG* in tumors but not correlated in normal lung tissues (Supplementary Fig. S7D), indicating that *MIR22HG* may inhibit tumor growth/cell cycle/proliferation in primary tumors. Upon further analysis of genes in the list, we found that increased MKI67 and other cell cycle/proliferation related genes, CHEK1, BIRC5 and BUB1, were significantly unfavorable for patient survival (Supplementary Figs. S7E and S7F).

***MIR22HG*, CDKN1A (p21), YBX1 and MET mRNA expression in primary tumors and correlation on different lung RNA-seq datasets**

We found MET mRNAs were decreased by 34%–46% after *MIR22HG* knockdown in 5 lung cancer cell lines (Fig. 4D). p21 mRNAs were increased by 20%–40% in H2228, PC9 and H1975 cells, while no changing in H1299 and H838 cells (Fig. 4F). This indicating *MIR22HG* regulates MET at the transcription level in all cells, while p21 only in a sub set of cells. In order to evaluate if this status found *in vitro* is also presented in primary tissues, we analyzed the *MIR22HG*, CDKN1A (p21), YBX1 and MET mRNA expression (Supplementary Figs. S8A and S8B) and performed the Pearson correlation analysis between *MIR22HG* and *MET* or *p21* mRNA in multiple lung RNA-seq data sets (total 1096 samples) including normal, tumor, as well as lung cancer cell lines. We did find a significantly positive correlation between *MIR22HG* and *MET* mRNA in two sets of lung

cancer cell lines (Supplementary Figs. S8C and S8D), but we didn't find a significant correlation between *MIR22HG* and *MET* mRNA in normal and tumor tissues (Supplementary Fig. S8C). A possible reason may be the tumor microenvironment affecting *MIR22HG* in regulating *MET* expression. Further investigations of the correlation between *MIR22HG* and *MET* protein on tissue array is warranted.

Regarding the correlation between *MIR22HG* and *p21* mRNA, we didn't find a significant correlation in both primary tumor and cell lines (Supplementary Fig. S8C), which is constant with our finding *MIR22HG* affects *p21* mRNA expression in a sub sets of tumor cells. To our surprise, *MIR22HG* is significantly correlated to *p21* mRNA in two sets of normal lung tissues (Supplementary Figs. S8C and S8E), indicating *MIR22HG* may positively regulate *p21* at the transcription level in normal lung tissues.

Higher expression of p21 mRNA is related to poor patient survival, and p21 protein is correlated with Ki-67 in a subset of primary lung tumors

Clinical studies of the presence of p21 in tumors have yielded divergent findings regarding its roles in cancer. Clinically, elevated levels of p21 have been detected in many human tumors associated with poor survival (gliomas, prostate, cervical, ovarian, and esophageal), while in other tumors (breast, gastric, and ovarian), loss of p21 expression has been associated with poor prognosis and decreased overall survival (33). We evaluated the association of p21 mRNA and patient survival in the Shedden et al. dataset which includes 442 LUADs. Kaplan-Meier survival curve and log-rank tests showed that higher expression levels of p21 mRNA were significantly correlated with poor patient outcome ($p = 0.04$) (Supplementary Fig. S9A). We have previously found the cell proliferation was decreased upon p21 knockdown in lung cancer cell lines. Takeshima et al. (43) reported that p21 protein expression was significantly positively correlated with ki-67 expression but not with p53 expression in 91 lung adenocarcinomas using immunohistochemical staining (IHC), suggesting that p21 may be involved in tumor cell proliferation. In order to confirm the p21 expression and tumor proliferation in lung cancer tissues, we performed IHC of p21 and proliferation marker ki-67 on tumor tissue array (TMA) containing 97 lung adenocarcinomas (Supplementary Figs. S9B–M). Approximately 25% of tumors show positive staining for both p21 and ki-67 in the cytoplasm or nucleus. These results indicate that p21 may promote tumor growth in a subset of lung cancer.

Discussion

Recently, a number of lncRNAs have been identified and characterized as important factors in fundamental physiological and pathological processes (10,11,44). LncRNAs play essential roles as either tumor suppressors or oncogenes, but only a small proportion of lncRNAs have been well characterized (45). In this study, we found that *MIR22HG* was significantly down-regulated in lung cancer, and decreased expression was associated with poor patient survival. *MIR22HG* can bind and stabilize YBX1 protein. Silencing of *MIR22HG* triggered YBX1 degradation by the proteasome and decreased *MET* mRNA/protein expression through promoter regulation by YBX1. Whereas, p21 mRNA and/or protein expression may be regulated by *MIR22HG* partially via YBX1 or *MET*. *MIR22HG*

may play a tumor suppressor role through regulation of cell cycle related genes in primary tumors.

As a master regulator of cancer cell biology, YBX1 is involved in all of Hanahan's 'hallmarks of cancer' (28,46). The YBX1 protein performs its functions both in the cytoplasm (role as RNA binding protein) and in the cell nucleus (role as a transcription factor) (27,47). We found YBX1 could affect cell proliferation in a sub set of tumor cells including EGFR mutated cells (PC-9 and H1975). Nuclear YBX1 has been reported to promote MET expression by directly binding to MET promoter in basal-like breast cancers (26). In consistent with *MIR22HG*, we found that both protein and mRNA of MET were decreased after YBX1 knockdown) indicating YBX1 regulates MET expression at the transcription level. Further, promoter luciferase assay and CHIP-PCR experiment are warranted. YBX1 accumulates in the centrosome during the mitotic phase (31). YBX1 could transition from the cytoplasm to the nucleus in the following cases: at G1/S phase interface, treatment with UV-radiation, DNA-damaging agents, upon oxidative stress hyperthermia, interaction with SRp30c and TP53 (47). We found the YBX1 protein was present in both the cytoplasm and nucleus, and accumulates in nucleus at mitosis in control cells (Supplementary Fig. S5A). The nuclear and cytoplasmic YBX1 proteins were significantly decreased upon *MIR22HG* knockdown indicating that *MIR22HG* may not only affect YBX1 degradation, but also affect YBX1 nuclear translocation.

Several genes are reported to display two separate roles in cancer, acting as either tumor suppressors or oncogenes including Myc, E2F1, AMPK, SIRT1, TGFb1, p38a, Notch pathway, Wnt pathway and p21 (40). The two-face role of p21 in regulating proliferation (cell cycle) and anti-apoptosis during different cell stages, e.g. cell cycle arrest in early staged and promotion of cell growth with higher levels of genomic instability at later stages, especially in TP53-deficient environment (40,48). We have found that p21 is a strong oncogene that could promote tumor growth through cell cycle regulation, apoptosis inhibition, and senescence promotion. We also found that CCNE1 protein was increased after *MIR22HG* knockdown, while decreased upon p21 knockdown, indicating that up-regulation of CCNE1 may also contribute to increased cell proliferation by *MIR22HG* knockdown. This result demonstrates that increased cell growth by *MIR22HG* knockdown may be partially through p21 anti-apoptosis effects and promote cell proliferation in lung cancer. We have found that approximately 25% of primary tumors show positive staining for both p21 and ki-67 in the cytoplasm or nucleus indicating that p21 may promote tumor growth in a subset of lung cancers. Our results indicate that the oncogenic role of p21 in lncRNA-mediated regulatory mechanism may provide a new therapeutic strategy.

An interesting observation was that cell cycle was arrested at 48 hrs after *MIR22HG* siRNA transfection, while cell proliferation was increased at 96–120 hrs after *MIR22HG* knockdown although we found that cell proliferation was not changed significantly at 48 hrs. A potential reason may be related to the two roles of p21 in regulating proliferation (cell cycle) and anti-apoptosis in different cell stages, e.g. cell cycle arrest at early stages and promotion of cell growth at late stages as reported by Georgakilas (48) and Galanos (40). We also found silencing of *MIR22HG* increased cell senescence at 48 h (Supplementary Figs. S6I and S6J), and cell senescence usually occurs in cycle arrested status (49). Other possible

reasons may be due to the increased oncogene *CCNE1* expression after *MIR22HG* knockdown (Fig. 6F) since overexpressed *CCNE1* could shorten the length of the G1 cell cycle phase, leading to aberrant origin firing and DNA replication stress and promotion of cell proliferation (50).

The evidence provided by this study suggests a model in which ultimate cell survival or death triggered by *MIR22HG* knockdown in lung cancer is determined by two levels of balance at the cellular and molecular levels. The cellular level reflects a balance of the phenotypes of cell proliferation/cell cycle, apoptosis, and senescence, and the molecular level reflects the balance of the expression levels and roles of several oncogenes including *YBX1*, *MET*, *p21*, *CCNE1* and *Myc*, etc. triggered by lncRNA *MIR22HG* (Fig. 7B). In primary tumors with a changing microenvironment, even more oncogene/cell cycle related genes change the balance causing either tumor growth or death (Supplementary Figs. S7A–F).

In conclusion, this study demonstrates that *MIR22HG* is a potential tumor suppressor which acts through binding and stabilizing *YBX1*, thereby regulating multiple cell survival/death signals including cell proliferation, apoptosis, and senescence by targeting oncogenes *MET* and *p21*. *MIR22HG* has potential as a new diagnostic/prognostic marker and a therapeutic target for lung cancer treatment.

Supplementary Material

Refer to Web version on PubMed Central for supplementary material.

Acknowledgments

This work was supported in part by the National Institutes of Health (grant R01CA154365 to D.G. Beer and A.M. Chinnaiyan; grant U01CA157715 to D.G. Beer; grant R21CA205414 to G. Chen), the University of Michigan's Cancer Center Support Grant (P30 CA46592), University of Michigan's Cancer Center Thoracic Oncology Program Research Grant (G. Chen), a University of Michigan Department of Surgery RAC grant (G. Chen), and the National Natural Science Foundation of China (NSFC) (81660324 to S. Feng; 81702270 to W. Su).

References

1. Siegel RL, Miller KD, Jemal A. Cancer Statistics, 2017. *CA Cancer J Clin.* 2017; 67:7–30. [PubMed: 28055103]
2. Janku F, Stewart DJ, Kurzrock R. Targeted therapy in non-small-cell lung cancer--is it becoming a reality? *Nat Rev Clin Oncol.* 2010; 7:401–14. [PubMed: 20551945]
3. Reck M, Heigener DF, Mok T, Soria JC, Rabe KF. Management of non-small-cell lung cancer: recent developments. *Lancet.* 2013; 382:709–19. [PubMed: 23972814]
4. Ma XL, Xiao ZL, Liu L, Liu XX, Nie W, Li P, et al. Meta-analysis of Circulating Tumor Cells as a Prognostic Marker in Lung Cancer. *Asian Pac J Cancer P.* 2012; 13:1137–44.
5. Han B, Park D, Li R, Xie M, Owonikoko TK, Zhang G, et al. Small-Molecule Bcl2 BH4 Antagonist for Lung Cancer Therapy. *Cancer Cell.* 2015; 27:852–63. [PubMed: 26004684]
6. Calin GA, Liu CG, Ferracin M, Hyslop T, Spizzo R, Sevignani C, et al. Ultraconserved regions encoding ncRNAs are altered in human leukemias and carcinomas. *Cancer Cell.* 2007; 12:215–29. [PubMed: 17785203]
7. Du Z, Fei T, Verhaak RG, Su Z, Zhang Y, Brown M, et al. Integrative genomic analyses reveal clinically relevant long noncoding RNAs in human cancer. *Nat Struct Mol Biol.* 2013; 20:908–13. [PubMed: 23728290]

8. Prensner JR, Chinnaiyan AM. The emergence of lncRNAs in cancer biology. *Cancer Discov.* 2011; 1:391–407. [PubMed: 22096659]
9. Trimarchi T, Bilal E, Ntziachristos P, Fabbri G, Dalla-Favera R, Tsigos A, et al. Genome-wide mapping and characterization of Notch-regulated long noncoding RNAs in acute leukemia. *Cell.* 2014; 158:593–606. [PubMed: 25083870]
10. Ma MZ, Chu BF, Zhang Y, Weng MZ, Qin YY, Gong W, et al. Long non-coding RNA CCAT1 promotes gallbladder cancer development via negative modulation of miRNA-218-5p. *Cell Death Dis.* 2015; 6:e1583. [PubMed: 25569100]
11. Tang J, Zhuo H, Zhang X, Jiang R, Ji J, Deng L, et al. A novel biomarker Linc00974 interacting with KRT19 promotes proliferation and metastasis in hepatocellular carcinoma. *Cell Death Dis.* 2014; 5:e1549. [PubMed: 25476897]
12. Clark MB, Mattick JS. Long noncoding RNAs in cell biology. *Semin Cell Dev Biol.* 2011; 22:366–76. [PubMed: 21256239]
13. Gutschner T, Diederichs S. The hallmarks of cancer: a long non-coding RNA point of view. *RNA Biol.* 2012; 9:703–19. [PubMed: 22664915]
14. Han L, Zhang EB, Yin DD, Kong R, Xu TP, Chen WM, et al. Low expression of long noncoding RNA PANDAR predicts a poor prognosis of non-small cell lung cancer and affects cell apoptosis by regulating Bcl-2. *Cell Death Dis.* 2015; 6:e1665. [PubMed: 25719249]
15. Kong R, Zhang EB, Yin DD, You LH, Xu TP, Chen WM, et al. Long noncoding RNA PVT1 indicates a poor prognosis of gastric cancer and promotes cell proliferation through epigenetically regulating p15 and p16. *Mol Cancer.* 2015; 14:82. [PubMed: 25890171]
16. Balbin OA, Malik R, Dhanasekaran SM, Prensner JR, Cao X, Wu YM, et al. The landscape of antisense gene expression in human cancers. *Genome Res.* 2015; 25:1068–79. [PubMed: 26063736]
17. Iyer MK, Niknafs YS, Malik R, Singhal U, Sahu A, Hosono Y, et al. The landscape of long noncoding RNAs in the human transcriptome. *Nat Genet.* 2015; 47:199–208. [PubMed: 25599403]
18. Wang L, He Y, Liu W, Bai S, Xiao L, Zhang J, et al. Non-coding RNA LINC00857 is predictive of poor patient survival and promotes tumor progression via cell cycle regulation in lung cancer. *Oncotarget.* 2016; 7:11487–99. [PubMed: 26862852]
19. Okayama H, Kohno T, Ishii Y, Shimada Y, Shiraishi K, Iwakawa R, et al. Identification of genes upregulated in ALK-positive and EGFR/KRAS/ALK-negative lung adenocarcinomas. *Cancer Res.* 2012; 72:100–11. [PubMed: 22080568]
20. Shedden K, Taylor JM, Enkemann SA, Tsao MS, Yeatman TJ, et al. Director's Challenge Consortium for the Molecular Classification of Lung A. Gene expression-based survival prediction in lung adenocarcinoma: a multi-site, blinded validation study. *Nat Med.* 2008; 14:822–7. [PubMed: 18641660]
21. Irizarry RA, Hobbs B, Collin F, Beazer-Barclay YD, Antonellis KJ, Scherf U, et al. Exploration, normalization, and summaries of high density oligonucleotide array probe level data. *Biostatistics.* 2003; 4:249–64. [PubMed: 12925520]
22. Seo JS, Ju YS, Lee WC, Shin JY, Lee JK, Bleazard T, et al. The transcriptional landscape and mutational profile of lung adenocarcinoma. *Genome Res.* 2012; 22:2109–19. [PubMed: 22975805]
23. Cancer Genome Atlas Research N. Comprehensive molecular profiling of lung adenocarcinoma. *Nature.* 2014; 511:543–50. [PubMed: 25079552]
24. Dhanasekaran SM, Balbin OA, Chen G, Nadal E, Kalyana-Sundaram S, Pan J, et al. Transcriptome meta-analysis of lung cancer reveals recurrent aberrations in NRG1 and Hippo pathway genes. *Nature communications.* 2014; 5:5893.
25. Huang da W, Sherman BT, Lempicki RA. Systematic and integrative analysis of large gene lists using DAVID bioinformatics resources. *Nat Protoc.* 2009; 4:44–57. [PubMed: 19131956]
26. Finkbeiner MR, Astanehe A, To K, Fotovati A, Davies AH, Zhao Y, et al. Profiling YB-1 target genes uncovers a new mechanism for MET receptor regulation in normal and malignant human mammary cells. *Oncogene.* 2009; 28:1421–31. [PubMed: 19151767]
27. Goodarzi H, Liu X, Nguyen HC, Zhang S, Fish L, Tavazoie SF. Endogenous tRNA-Derived Fragments Suppress Breast Cancer Progression via YBX1 Displacement. *Cell.* 2015; 161:790–802. [PubMed: 25957686]

28. Lasham A, Print CG, Woolley AG, Dunn SE, Braithwaite AW. YB-1: oncoprotein, prognostic marker and therapeutic target? *Biochem J.* 2013; 449:11–23. [PubMed: 23216250]
29. Kishikawa T, Otsuka M, Yoshikawa T, Ohno M, Ijichi H, Koike K. Satellite RNAs promote pancreatic oncogenic processes via the dysfunction of YBX1. *Nat Commun.* 2016; 7:13006. [PubMed: 27667193]
30. Sorokin AV, Selyutina AA, Skabkin MA, Guryanov SG, Nazimov IV, Richard C, et al. Proteasome-mediated cleavage of the Y-box-binding protein 1 is linked to DNA-damage stress response. *The EMBO journal.* 2005; 24:3602–12. [PubMed: 16193061]
31. Kawaguchi A, Asaka MN, Matsumoto K, Nagata K. Centrosome maturation requires YB-1 to regulate dynamic instability of microtubules for nucleus reassembly. *Sci Rep.* 2015; 5:8768. [PubMed: 25740062]
32. Cohen AA, Kalisky T, Mayo A, Geva-Zatorsky N, Danon T, Issaeva I, et al. Protein dynamics in individual human cells: experiment and theory. *PLoS One.* 2009; 4:e4901. [PubMed: 19381343]
33. Abbas T, Dutta A. p21 in cancer: intricate networks and multiple activities. *Nat Rev Cancer.* 2009; 9:400–14. [PubMed: 19440234]
34. Parveen A, Akash MS, Rehman K, Kyunn WW. Dual Role of p21 in the Progression of Cancer and Its Treatment. *Crit Rev Eukaryot Gene Expr.* 2016; 26:49–62. [PubMed: 27278885]
35. El-Deiry WS. p21(WAF1) Mediates Cell-Cycle Inhibition, Relevant to Cancer Suppression and Therapy. *Cancer Res.* 2016; 76:5189–91. [PubMed: 27635040]
36. Chang BD, Watanabe K, Broude EV, Fang J, Poole JC, Kalinichenko TV, et al. Effects of p21Waf1/Cip1/Sdi1 on cellular gene expression: implications for carcinogenesis, senescence, and age-related diseases. *Proc Natl Acad Sci U S A.* 2000; 97:4291–6. [PubMed: 10760295]
37. Roninson IB. Oncogenic functions of tumour suppressor p21(Waf1/Cip1/Sdi1): association with cell senescence and tumour-promoting activities of stromal fibroblasts. *Cancer Lett.* 2002; 179:1–14. [PubMed: 11880176]
38. Liu R, Wettersten HI, Park SH, Weiss RH. Small-molecule inhibitors of p21 as novel therapeutics for chemotherapy-resistant kidney cancer. *Future Med Chem.* 2013; 5:991–4. [PubMed: 23734682]
39. Orend G, Hunter T, Ruoslahti E. Cytoplasmic displacement of cyclin E-cdk2 inhibitors p21Cip1 and p27Kip1 in anchorage-independent cells. *Oncogene.* 1998; 16:2575–83. [PubMed: 9632134]
40. Galanos P, Vougas K, Walter D, Polyzos A, Maya-Mendoza A, Haagensen EJ, et al. Chronic p53-independent p21 expression causes genomic instability by deregulating replication licensing. *Nat Cell Biol.* 2016; 18:777–89. [PubMed: 27323328]
41. Noda A, Ning Y, Venable SF, Pereira-Smith OM, Smith JR. Cloning of senescent cell-derived inhibitors of DNA synthesis using an expression screen. *Exp Cell Res.* 1994; 211:90–8. [PubMed: 8125163]
42. Wang Y, Blandino G, Givol D. Induced p21 waf expression in H1299 cell line promotes cell senescence and protects against cytotoxic effect of radiation and doxorubicin. *Oncogene.* 1999; 18:2643–9. [PubMed: 10353608]
43. Takeshima Y, Yamasaki M, Nishisaka T, Kitaguchi S, Inai K. p21WAF1/CIP1 expression in primary lung adenocarcinomas: heterogeneous expression in tumor tissues and correlation with p53 expression and proliferative activities. *Carcinogenesis.* 1998; 19:1755–61. [PubMed: 9806155]
44. Wang Y, He L, Du Y, Zhu P, Huang G, Luo J, et al. The long noncoding RNA lncTCF7 promotes self-renewal of human liver cancer stem cells through activation of Wnt signaling. *Cell Stem Cell.* 2015; 16:413–25. [PubMed: 25842979]
45. Qi P, Du X. The long non-coding RNAs, a new cancer diagnostic and therapeutic gold mine. *Mod Pathol.* 2013; 26:155–65. [PubMed: 22996375]
46. Hanahan D, Weinberg RA. Hallmarks of cancer: the next generation. *Cell.* 2011; 144:646–74. [PubMed: 21376230]
47. Eliseeva IA, Kim ER, Guryanov SG, Ovchinnikov LP, Lyabin DN. Y-box-binding protein 1 (YB-1) and its functions. *Biochemistry Biokhimiia.* 2011; 76:1402–33. [PubMed: 22339596]
48. Georgakilas AG, Martin OA, Bonner WM. p21: A Two-Faced Genome Guardian. *Trends in molecular medicine.* 2017; 23:310–9. [PubMed: 28279624]

49. Blagosklonny MV. Cell cycle arrest is not senescence. *Aging*. 2011; 3:94–101. [PubMed: 21297220]
50. Macheret M, Halazonetis TD. Intragenic origins due to short G1 phases underlie oncogene-induced DNA replication stress. *Nature*. 2018; 555:112–6. [PubMed: 29466339]

Author Manuscript

Author Manuscript

Author Manuscript

Author Manuscript

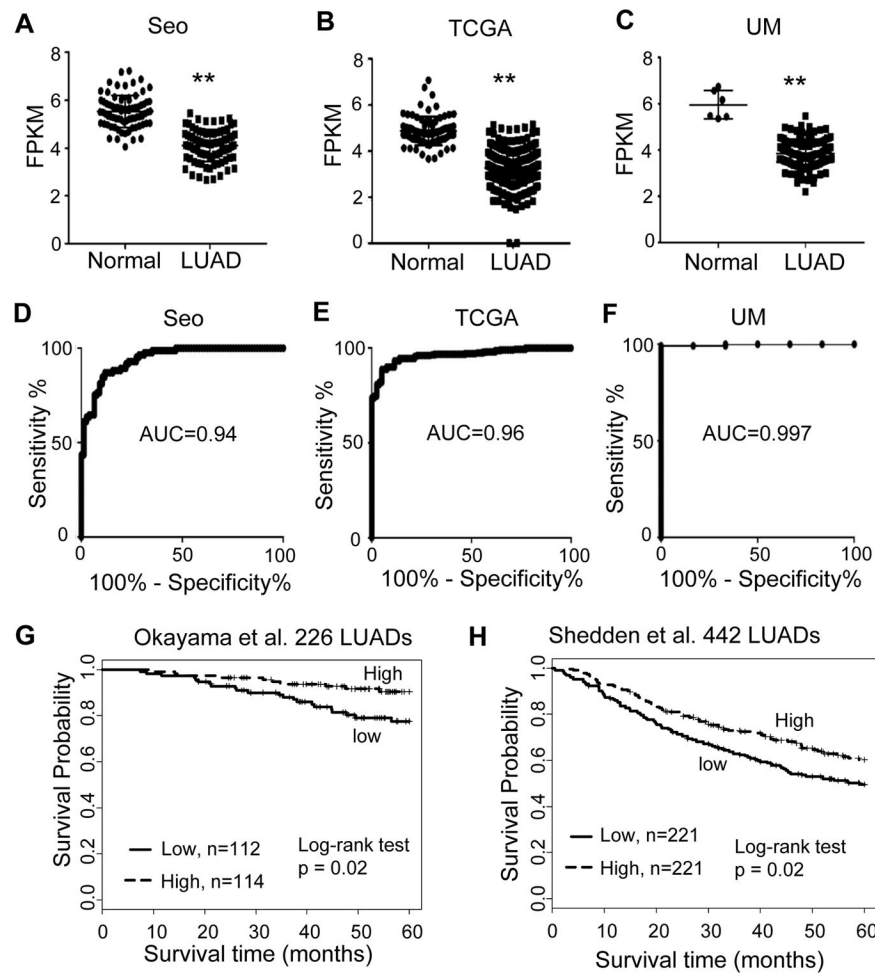


Figure 1. Differential expression of long Non-coding RNA *MIR22HG* in LUADs and correlated to patient survival

(A–C) Scatter plots of *MIR22HG* expression levels in LUAD and normal tissue samples in Seo, TCGA and UM RNA-Seq datasets (y-axis is log₂ of FPKM value, ** LUAD vs. Normal, $p < 0.001$ in all 3 data sets). (D–F) ROC curves with AUC values of *MIR22HG* in Seo (85 LUAD vs 77 N), TCGA (312 LUAD vs 79 N) and UM (67 LUAD vs 6 N) RNA-Seq data sets. (G and H) Kaplan-Meier survival curves with log-rank test of *MIR22HG* in the Okayama (226 LUADs) and Shedden (442 LUADs) data sets. Lower *MIR22HG* expression (median as cutoff value) was significantly correlated with poor patient survival.

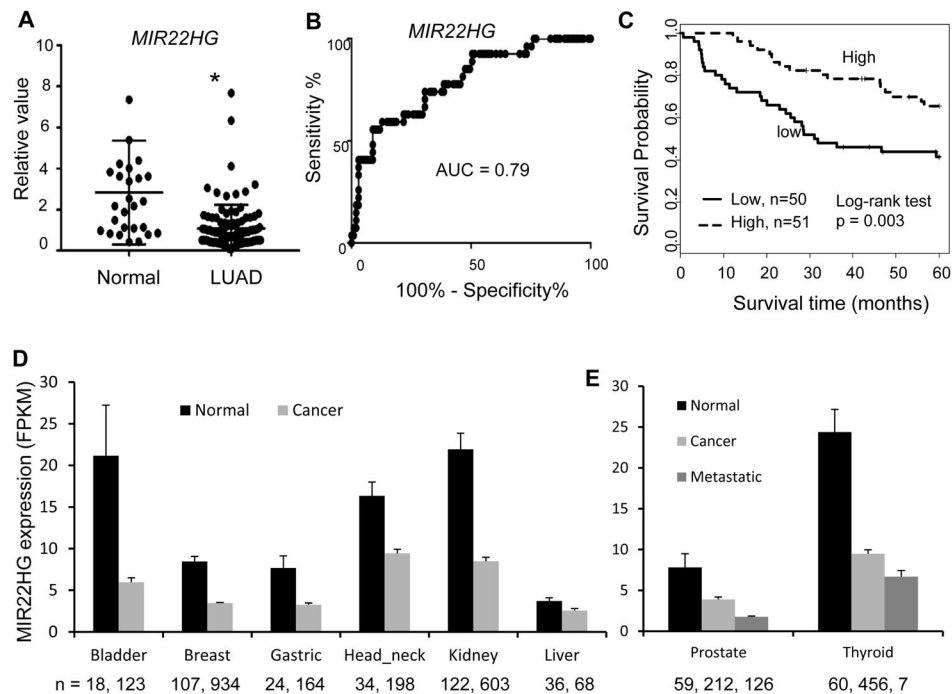


Figure 2. Validation of *MIR22HG* expression pattern in an independent cohort of LUADs and expression pattern in other types of cancer

(A) Scatter plot indicating *MIR22HG* expression was lower in tumor (measured by RT-PCR, y-axis is fold change to mean of all tissues, ACTB is used as loading control, * LUAD vs. normal, $p < 0.01$ by t test). (B) ROC curve indicated an excellent AUC (0.79) for classifying the 101 LUAD from 27 normal lung tissues based on *MIR22HG* expression. (C) Kaplan-Meier survival curve indicated lower *MIR22HG* expression was unfavorable for patient survival. (D – E) Comparison of *MIR22HG* expression in cancers and matched normal tissues (mean + SEM, log₂ of FPKM from RNA-seq data). Case number of each tissue is indicated. The original data was downloaded from MiTranscriptome with modification.

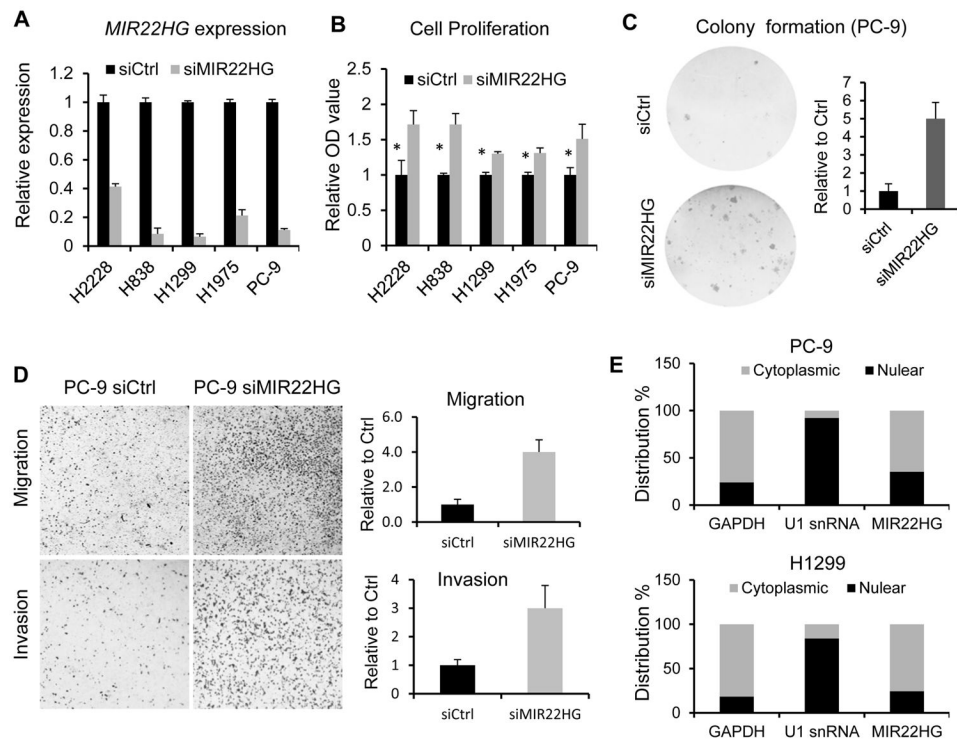


Figure 3. *MIR22HG* acts as tumor suppressor role in lung cancer

(A) *MIR22HG* siRNA knockdown efficiency (48 h) in PC-9, H1975, H2228, H1299 and H838 cells measured by qRT-PCR. GAPDH is used as loading control. (B) Cell proliferation is increased after *MIR22HG* siRNAs treatment in PC-9, H1975, H2228, H1299 and H838 cell lines. * $p < 0.05$ by t test. (C) Colony formation is increased after *MIR22HG* siRNA transfection on PC-9 cell line. The right figure is the relative quantified value. (D) Silencing of *MIR22HG* by siRNA increases cellular invasion and migration ability in PC-9 cell lines (4X). The right figures are the relative quantified value. (E) qRT-PCR showing the nuclear and cytoplasmic fractions of *MIR22HG* in PC-9 and H1299 cells. GAPDH is used as cytoplasmic control and U1 snRNA as nuclear control. *MIR22HG* is primarily in cytoplasm (61% – 76%).

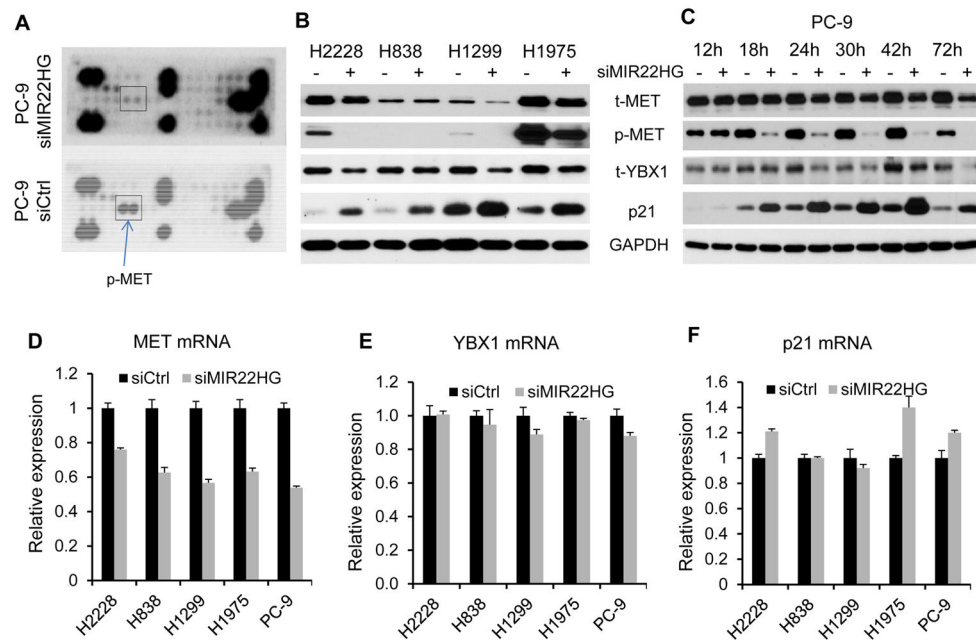


Figure 4. *MIR22HG* knockdown decreases YBX1 and MET, but increases p21 expression
 (A) The whole blot of Receptor tyrosine kinases (RTK) protein array. Phosphor MET was decreased after *MIR22HG* knockdown by siRNAs. (B) MET and YBX1 proteins were decreased, whereas p21 protein increased after *MIR22HG* knockdown by siRNAs in H2228, H838, H1299 and H1975 cells. (C) MET, YBX1 and p21 proteins were altered as early as 18–24 hrs after *MIR22HG* knockdown by siRNAs in PC-9 cells. (D–F) Changing of the mRNA expression on MET (D), YBX1 (E) and p21 (F) after *MIR22HG* knockdown at 48 h in PC-9, H1975, H2228, H1299 and H838 cell lines. GAPDH is used as loading control.

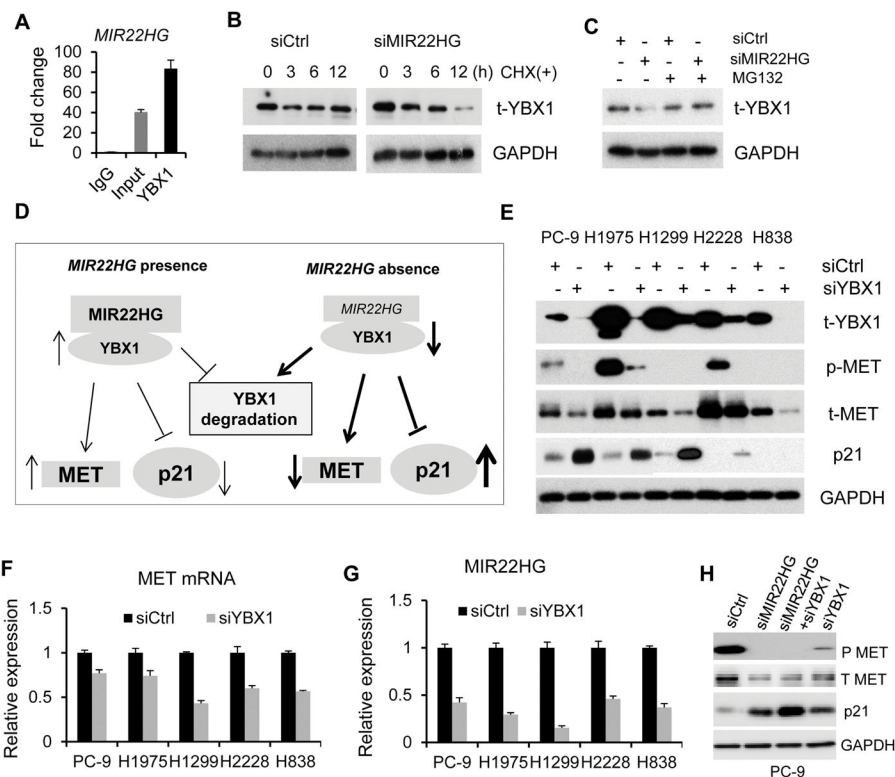


Figure 5. *MIR22HG* interacts with YBX1 protein

(A) *MIR22HG* expression (80 fold change as compared to IgG) by qRT-PCR from RIP assay. (B) Western blot showing the change in YBX1 expression affected by CHX treatment after *MIR22HG* knockdown. (C) Western blot of YBX1 expression in control and *MIR22HG* knockdown cells treated with, or without MG132. (D) Graphic model of the presence and absence of *MIR22HG*. *MIR22HG* binds and stabilizes the YBX1 protein, and acts through a *MIR22HG*-YBX1 complex to promote MET and inhibit p21 expression. (E) The protein expression of YBX1, MET and p21 after YBX1 siRNA treatment at 72 h in PC-9, H1975, H1299, H838 and H2228 cells by western blot. (F, G) Changes in mRNA expression for MET (F) and *MIR22HG* (G) upon YBX1 knockdown by siRNA at 48 h in lung cancer cells measured by qRT-PCR. GAPDH is used as loading control. (H) Western blot showing the changes in MET and p21 expression affected by *MIR22HG* and YBX1 knockdown.

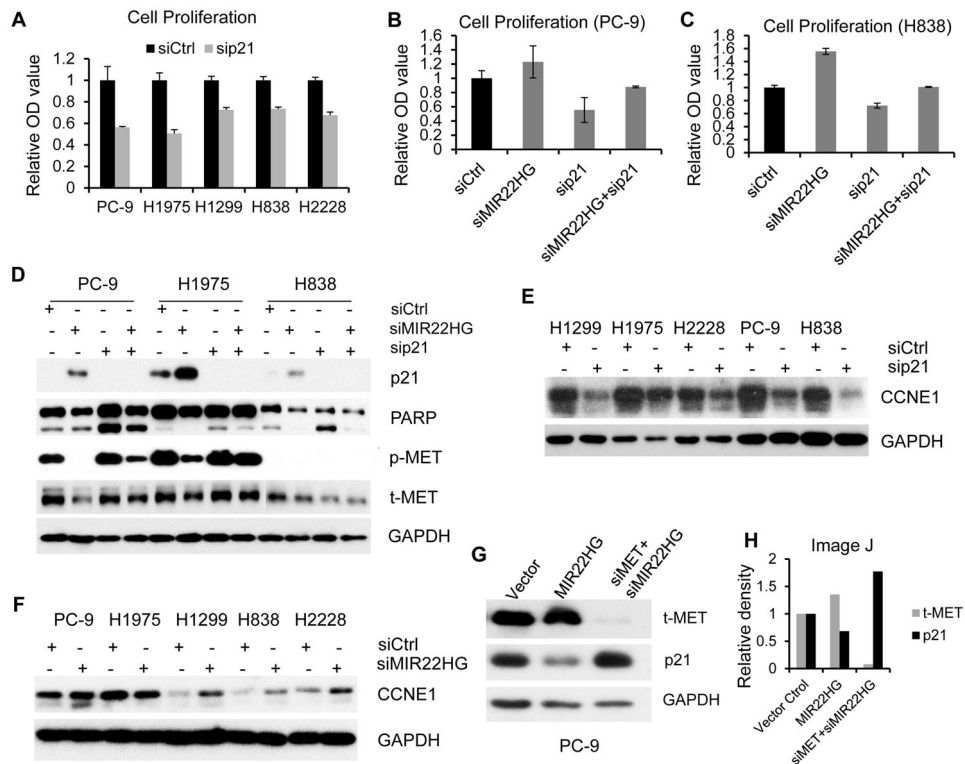


Figure 6. p21 plays an oncogenic role in promoting tumor cell proliferation and anti-apoptosis (A) Cell proliferation decreased after *p21* siRNAs treatment in PC-9, H1975, H2228, H1299 and H838 cell lines at 96 h – 120 h measured by WST-1 assay. (B and C) Changes in cell proliferation after *MIR22HG*, *p21* or both siRNAs treatment in PC-9 and H838 at 96 h measured by WST-1 assay. (D) The protein expression of cleaved PARP after *MIR22HG*, *p21* or both siRNAs treatment in PC-9, H1975 and H838 cells measured by western blot. (E and F) CCNE1 protein expression after *p21* siRNA (E) and *MIR22HG* siRNA (F) treatment at 72 h in lung cancer cells. (G) Western blot showing the total MET and *p21* proteins expression after transfection of *MIR22HG* over expression construct or both siRNAs of MET and *MIR22HG*. (H) Quantitative value of image G by Image J.

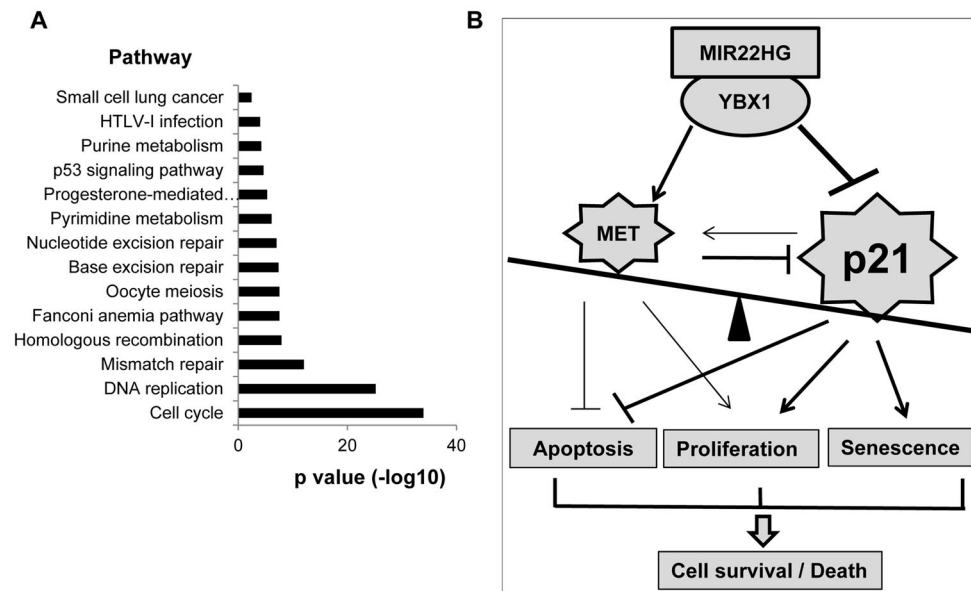


Figure 7. Genes negatively correlated to *MIR22HG* are involved in cell cycle/proliferation regulation in primary lung cancer, and the schematic model of the role of *MIR22HG* in lung cancer

(A) David gene pathway analysis of 444 *MIR22HG* negatively correlated coding genes ($r < -0.35$, $p < 0.001$). Cell cycle/proliferation related signaling is significantly involved. (B) The schematic model of the cell survival/death signaling regulated by YBX1, MET, p21 triggered by *MIR22HG* knockdown in lung cancer. The final cell survival or death triggered by *MIR22HG* knockdown is determined by two levels of rebalancing from cellular and molecular signals. Line weight represents the relevant effect of either inhibition or stimulation (arrow). In this study, p21 was strongly inhibited by both *MIR22HG*/YBX1 and MET, while MET was strongly stimulated by *MIR22HG*. The potential weak feedback role among these proteins is also presented.